Collisional destruction of fast H_3^+ ions in noble gases

W. Wolff, L. F. S. Coelho, and H. E. Wolf
Instituto de Física, Universidade Federal do Rio de Janeiro, Caixa Postal 68528, 21945 Rio de Janeiro, Rio de Janeiro, Brazil

N. V. de Castro Faria
Departamento de Física, Pontifícia Universidade Católica do Rio de Janeiro, Caixa Postal 38071, 22453 Rio de Janeiro, Rio de Janeiro, Brazil

(Received 19 October 1990; revised manuscript received 4 December 1990)

We have measured the total destruction cross sections for H_3^+ ions colliding with He, Ne, Ar, and Xe atoms in the velocity range from 2.5 to 7 atomic units (470 to 3700 keV). The collisional destruction cross section of D_3^+ ions by Ar atoms was also measured, and was found to be comparable to the H_3^+ values. The cross-section data were analyzed in two different ways. It was first established in a strictly empirical way that the cross sections for all noble gases may be scaled, in the energy range studied, by velocity-independent factors. In addition, the data were found to be suitably fitted by a semiempirical version of the free-collision model of Meron and Johnson [Phys. Rev. A **41**, 1365 (1990)].

PACS number(s): 34.90.+q

I. INTRODUCTION

The knowledge of the destruction cross sections for fast H_3^+ ions colliding with atoms is important for the study of several processes, such as fast H and H^- production. H_3^+ destruction through collisional dissociation produces fast negative beams [1] with yields much larger than those from H^+ or H_2^+ projectiles, being therefore a useful tool for the work with negative ions at accelerators with position high-voltage terminals. Otherwise, the destruction of H_3^+ is a subject interesting by itself. Because of the complex structure of the hydrogen molecular ion, there are no calculations of these cross sections from first principles. An approximate method for molecular destruction calculations has been used instead [2,3], its basis being a model usually employed for atomic electron stripping processes, the free-collision model. Recently a semiempirical version of this model, capable of generating electron stripping cross sections for fast H and H^-, was developed by Meron and Johnson [4] and achieved reasonable accuracy over a broad range of energies and target atomic numbers. Although H and H^- are much simpler systems than H_3^+, it is tempting to verify the applicability of this semiempirical model to this more complex situation. As only a few scattered measurements [1,5,6] of H_3^+ destruction cross sections have been published so far, a systematic study in a wide range of velocities and employing several targets is called for, and this is the main purpose of the present work.

In order to be able to measure meaningful H_3^+ destruction cross-section values, it is essential to have reproducible vibrational distributions of the H_3^+ ions leaving the ion source [7,8]. This also implies isotopic independent cross sections. H_3^+ and its several isotopomers (D_3^+,HD_2^+, etc.) posses equal electronic but different rovibrational structures, with smaller vibrational level spacings for larger atomic mass values [9]. Possible isotopic effects in the deexcitation transition rates [10] within the ion source may lead to different internal energies and excited-state distributions. This possibility was investigated comparing the H_3^+ and the D_3^+ destruction cross sections for an Ar target. However, owing to the much larger kinetic energies of the projectiles involved in the present work, the cross sections are not believed to be seriously affected by initial internal rovibrational excitations of the projectiles. In addition, the good reproducibility of our results and the absence of isotopic effects, as demonstrated in Secs. II and III, respectively, point to the prevalence of a stable vibrational distribution [11] and, consequently, to the reliability of the results.

II. EXPERIMENTAL APPARATUS AND METHODS

The attenuation of the H_3^+ beam was measured as a function of the pressure of a differentially pumped gas target and the total destruction cross section directly determined. The beam energy was in the 0.47–3.7-MeV range. Typical currents were hundreds of picoamperes. The H_3^+ beam was obtained from the PUC/RJ 4 MV Van de Graaff (HVEC) accelerator, employing its standard radio-frequency ion source.

After momentum analysis in a 90° magnet, the beam was collimated by a set of staggered crossed pairs of micrometric sliding slits, defining beam dimensions always smaller than 0.5×0.5 mm^2. The collimated beam passed through a diaphragm of 2-mm diam, before entering a large chamber containing the gas target, and left the chamber through a 5-mm diaphragm. Both diaphragms acted as vacuum impedances between the chamber and the beam line. Special care was taken to avoid the noncentral part of the beam, as it may contain fragments originated from the Coulomb explosion of the H_3^+ on the residual gas and/or the collimators. The beam, when drastically reduced by collimation, could be directly

detected and its composition checked by surface barrier detectors.

The gas target cell was 10 cm long, and fitted with entrance and exit apertures of 0.8 and 2.0 mm, respectively, A pressure gradient of nearly a factor 10^3 was maintained between the gas cell and the surrounding vacuum by a 4-in. diffusion pump, with a pumping speed of 200 l/s, mounted directly underneath the gas cell. The vacuum system also included two diffusion pumps installed along the beam line close to the entrance and the exit diaphragms. The gas-cell pressure was measured with a thermocouple device, separately calibrated for each gas against a McLeod gauge. This calibration was done in an independent experimental setup and, except for xenon, a liquid-nitrogen trap was used to condense possible contaminant gases and the mercury reservoir of the McLeod gauge was cooled to 0 °C in order to reduce backstreaming to the trap. The total uncertainty in the gas target thickness, arising from the absolute calibration of the McLeod gauge, the experimental fluctuations in the calibration, and the effective target length corrections, was estimated as 10%. The target gases nominal purities were 99.99%, high enough to ensure a negligible effect on the Ne, Ar, and Xe measurements. However, due to the small destruction cross section for He targets, the He data are more sensitive to impurities and fluctuations of the quality of the vacuum outside the gas cell. Preliminary measurements were also carried out with a krypton gas target, which unfortunately was not available during the later stages of the experiment.

The beam, after passing through the target chamber, was analyzed by a second magnet, and the H_3^+ current collected by a Faraday cup. The normalization of the data for equal amounts of incident H_3^+ ions was carried out by measuring the charge collected by a rotating beam chopper located 30 cm upstream the gas cell. The attenuation of the normalized transmitted charge as a function of the gas pressure determined, after fitting the data points by an exponential curve, the destruction cross section. The deviation of the experimental points from the exponential curve was always smaller than 5%.

Uncertainties in the absolute values of the cross sections arose from target thickness uncertainties, uncertainties in the measured beam current, gas purity, vacuum quality, and the fitting procedure. An average uncertainty of ±15% must be assigned to the absolute cross sections measured in this work.

Systematic destruction cross-section measurements were made by varying the source conditions in several ways. In order to quench the excited states inside the ion source [12], a mixture of 1:10 hydrogen to helium was employed in a trial experiment but this did not produce results different from those obtained with pure H_2 gas. The same was true for different and extreme pressures and extraction conditions of the source. Careful checks were also made in order to ensure the good day-to-day reproducibility of the data.

III. RESULTS AND DISCUSSION

A. Empirical approach

The experimental destruction cross sections of H_3^+ incident on noble gases are presented in Table I, as well as the D_3^+ data for an argon target. Results obtained by other authors are also included. D_3^+ data were obtained for a few velocities only, this restriction being imposed by reasons of radiation protection.

Two main features can be extracted from Table I. First, the present results compare well with the ones obtained by other authors (for D_3^+ there are no previous published data available). Second, the cross sections for H_3^+ and D_3^+ incident on argon, with the same velocities, are essentially the same, not showing any isotopic effect.

Since the destruction of a molecular ion such as H_3^+ is a hard problem to tackle theoretically, our first step in analyzing the data of Table I consisted in looking for a purely empirical representation of the several cross sections, for a given velocity, in terms of a simple geometrical parameter. To this end we tried to scale all cross sections according to

$$\sigma_{\text{gas}}(v)=F_{\text{gas}}\sigma_{\text{Ne}}(v) \ . \tag{1}$$

The neon cross sections were arbitrarily chosen as reference values, and the constants F_{gas} were assumed velocity independent. These constants were determined by dividing each cross-section value $\sigma_{\text{gas}}(v)$ by the corresponding

TABLE I. Collisional destruction cross sections of H_3^+ and D_3^+ (in units of 10^{-16} cm^2.

Velocity		Ne		Ar			
		This			This work		
v/v_0	He	work	Ref. [1]	Ref. [5]	H_3^+	D_3^+	Xe
2.5	1.34	3.43			6.17	6.04	7.25
3.0	1.06	2.87			5.42	5.80	6.90
3.5	0.62	2.40		4.68	4.72	4.89	6.68
4.0	0.73	2.18	1.9	4.10	4.33	4.46	5.96
4.5	0.76	2.02		3.80	3.99	3.97	5.39
5.0	0.49	1.80			3.52		5.15
5.5	0.36	1.54			3.31		4.93
6.0	0.35	1.50			3.03		4.76
6.5	0.24	1.32			2.57		4.29
7.0	0.34	1.09			2.26		3.79

TABLE II. H_3^+ destruction cross-section divided by the normalization constants F (in units of 10^{-16} cm^2).

v/v_0	$(\sigma/F)_{He}$	σ_{Ne}	$(\sigma/F)_{Ar}$	$(\sigma/F)_{Xe}$
2.5	4.5	3.4	3.1	2.5
3.0	3.6	2.9	2.7	2.4
3.5	2.1	2.4	2.4	2.3
4.0	2.5	2.2	2.2	2.1
4.5	2.6	2.0	2.0	1.9
5.0	1.6	1.8	1.8	1.8
5.5	1.2	1.5	1.7	1.7
6.0	1.2	1.5	1.5	1.7
6.5	0.8	1.3	1.3	1.5
7.0	1.1	1.1	1.1	1.3

value $\sigma_{Ne}(v)$ for neon and by subsequently averaging these ratios over all measured velocities. The normalized cross sections $\sigma_{gas}(v)/F_{gas}$ are presented in Table II and exhibit, for a given velocity except the lowest one, a remarkable constancy over all gases, thus indicating that a scaling procedure of the type (1) is indeed possible.

The first column of Table III contains the numerical values obtained for these empirical scaling factors F_{gas}, together with their standard deviations. The F were then compared in the second column of Table III to the squares of the Hartree-Fock radii $\langle r_{nl} \rangle^2$ (Table IV) of the most external subshell of the noble gases [13]. It is evident from this comparison that the squares of the Hartree-Fock radii did not provide a good parametrization for the constants F. Parametrizations with an arbitrary power of $\langle r_{nl} \rangle$ or Z also proved unsuccessful. Therefore we next tried to parametrize the F with an empirically determined power of the geometric radii of the target atoms (Table IV). These are the radii used in the kinetic theory of gases, and their values were taken from Ref. [14]. Surprisingly, the fourth power of the geometric radii provided a good parametrization, as can be seen from the third column of Table III. It should be mentioned at this point that this empirical "fourth power law" became evident already during the early stages of this work, when the krypton gas target was still available, and that the preliminary krypton data filled very well into this description. It should be pointed out that this finding is purely empirical and may not have any major physical significance, since one normally expects cross sections to scale with the square of some kind of atomic radius.

TABLE III. Normalization factors F and their comparison to the square of the Hartree-Fock radius $\langle r_{nl} \rangle^2$ of the most external noble-gas subshell and to the fourth power of the geometric radius R_g^4. The values of the radii are in atomic units.

Element	F	$F/\langle r_{nl} \rangle^2$	$F/R_g^4(10^{-3})$
He	0.30±0.07	0.35±0.07	10.7±2.5
Ne	1	1.06	11.7
Ar	1.98±0.09	0.72±0.03	11.5±0.5
Xe	2.87±0.40	0.52±0.07	11.0±1.5

TABLE IV. Compilation of the four types of noble-gas atomic radii that appear in this work: Hartree-Fock radii (Ref. [13]) $\langle r_{nl} \rangle$, Thomas-Fermi radii R_{TF}, geometric radii (Ref. [14]) R_g, as well as the radius parameter R of the formula of Meron and Johnson (Ref. [4]) as determined from the present data. All values are expressed in atomic units.

Element	$\langle r_{nl} \rangle$	R_{TF}	R_g	R
He	0.93	0.703	2.30	0.167
Ne	0.97	0.411	3.04	0.114
Ar	1.66	0.338	3.62	0.108
Xe	2.34	0.234	4.02	0.075

B. Free-collision model approach

The destruction of a molecular ion is usually proceeded by the molecule being excited to a self-dissociating electronic state. This process is described by approximations which, owing to the multicenter character of the molecular wave function and to the presence of the additional degrees of freedom of vibration and rotation, are more complex than those for the excitation of atomic electrons. In the high-velocity regime, however, it may be treated in a similar fashion.

The excitation of atomic electrons to the continuum, at projectile velocities much larger than the electron average orbital velocity, may be described by the free-collision model [4,15–17]. In this model, the incident projectile electron is considered free and having the same velocity of the projectile. Electron loss occurs if the energy transfered to this electron, as measured in the rest frame of the projectile, exceeds the ionization energy. This approach was first used by Salpeter [2] to describe the destruction of the molecular ion H_2^+, and a rough agreement with experiment was achieved. The constituents of H_2^+ were considered as free particles and the energy gained by the protons and the electron eventually led to vibrational or electronic excitation, respectively. The H_2^+ molecule was also assumed to be initially in its fundamental vibrational level.

This free-particle approach was improved by Berkner *et al.* [3], who calculated cross sections for each initial vibrational level of H_2^+ and averaged the results assuming two different vibrational distributions. This procedure, taking into account the excited vibrational levels, led to a good agreement with the experimental cross-section values also obtained by these authors.

Before proceeding to an application of the free-collision-model version of Meron and Johnson [4] to the present cross-section data, we first compare the cross section σ_D for the destruction of H_3^+ in neon with existing results [18] for the H^- electron detachment cross section $\sigma_{\bar{1}0}$ and the H(1s) electron-loss cross section σ_{01}. These comparisons are grounded on (a) the assumption of the free-collision model, that is, a projectile velocity much larger than the average orbital velocity of the electrons, and (b) the double electron loss being expected to be at least one order of magnitude less probable than the single electron loss, in a manner similar to another two-electron

projectile, the H^- ion [18] (both processes destroy either H^- or H_3^+).

Figure 1 displays these three cross sections. While they are of different magnitudes, as is to be expected, their velocity dependence is very similar. The first dissociative electronic state of H_3^+ is located ~ 19 eV above the ground state. This dissociation energy is considerably larger than the H^- ionization energy, since one of the H^- electrons is weakly bound (~ 1 eV). The larger momentum transfer needed for dissociation to occur causes σ_D to be systematically smaller than the corresponding $\sigma_{\bar{1}0}$ values. Since neutral hydrogen possesses an ionization energy more similar to the H_3^+ dissociation energy and has only a single electron, one expects σ_D to be roughly twice as large as σ_{01}, since removal of either electron on H_3^+ would destroy this ion. Indeed, an examination of the data of Fig. 2 indicates a very approximate relation between the three cross sections of $\sigma_{\bar{1}0} \sim 1.5\sigma_D \sim 2\sigma_{01}$.

Also presented in Figure 1 are the free-collision-model curves obtained by Meron and Johnson for the $\sigma_{\bar{1}0}$ and σ_{01} data. Since the atomic cases are well described by this model, as the quality of the fits shows, and since the velocity dependence of σ_D behaves in a similar way, one is encouraged to apply the model also to the ion H_3^+.

The simple analytical formula for electron loss in atomic systems developed by Meron and Johnson may be casted, after some rearrangements, into the following form (all quantities in atomic units):

$$\sigma = \frac{\sigma_0}{1+(2vR)^2}\frac{\Phi_1}{\Phi_2} QZ^{C_Q} , \tag{2a}$$

where v is the projectile velocity, Q and C_Q are parameters accounting for the excitation of the target, and R is a Z-dependent scaling radius (empirically found to be

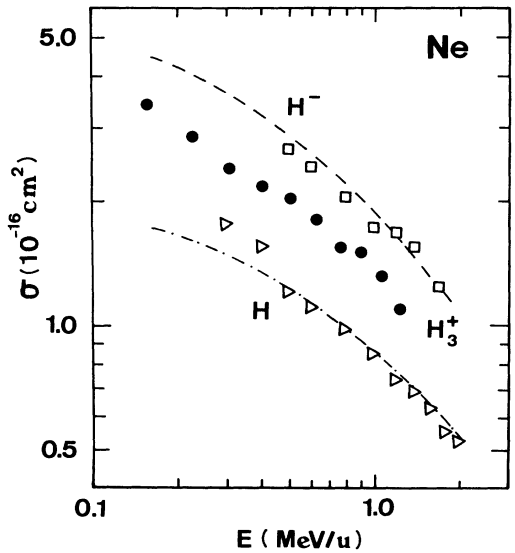

FIG. 1. Comparison between several cross sections for a neon target: ▷, $\sigma_{01}(H)$; □, $\sigma_{\bar{1}0}(H^-)$; ●, present values for $\sigma_D(H_3^+)$. The experimental data for H and H^- were taken from Ref. [18] and the theoretical curves came from Ref. [4].

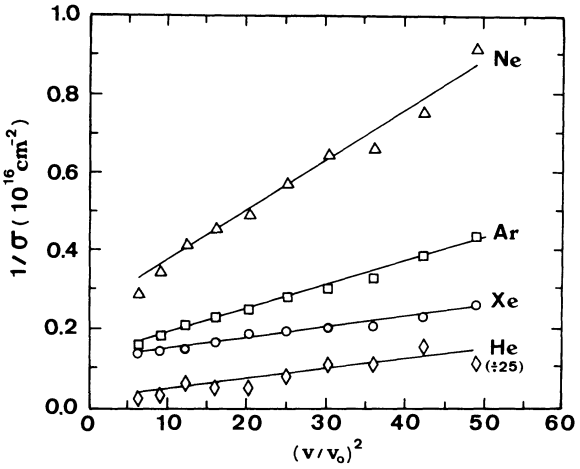

FIG. 2. Inverse cross sections for the destruction of H_3^+ ions colliding with several noble gases vs the square of the ion velocity $(v/v_0)^2$. The straight lines represent least-squares fits.

smaller than the Thomas-Fermi radius),

$$\sigma_0 = 16Z^2R^4 , \tag{2b}$$

$$\Phi_1 = 1-(v_i/2v)^2 , \tag{2c}$$

$$\Phi_2 = 1+(v_iR)^2 , \tag{2d}$$

and

$$v_i = (2E_0/m)^{1/2} . \tag{2e}$$

When the H_3^+ ion gains a minimum energy of 19.3 eV, it is excited from its rovibrational and electronic ground state to the $^1E'$ self-dissociative state. Taking from the statistical model [11] the average internal energy of the ions to be 1.5 eV, the minimum excitation energy E_0 becomes about 17.8 eV, and this value was used in the subsequent application of the formulas.

The following procedure was employed to fit the cross-section data of the present work to formulas (2). First the parameters Φ_1 and Φ_2 were set equal to unity, the justification for this arising from expressions (2c) and (2d). In fact, in the free-collision-model regime $v_i \ll v$, and, since R is not larger than the Thomas-Fermi radius, the product v_iR is also small. The inverse of the measured cross sections for the several noble gases was then plotted against v^2 in Fig. 2 and straight lines of the type $1/\sigma_{\text{gas}} = a_{\text{gas}} + b_{\text{gas}}v^2$ were separately fitted by a least-squares procedure to the data of each noble gas. In this way numerical values were obtained for the coefficients a and b for each noble gas. The various parameters appearing in formulas (2) are related to the coefficients a and b according to

$$R = \frac{1}{2}\left[\frac{b}{a}\right]^{1/2} , \tag{3a}$$

$$QZ^{C_Q} = \frac{a}{Z^2b^2} . \tag{3b}$$

Numerical values for the parameters R (listed in Table

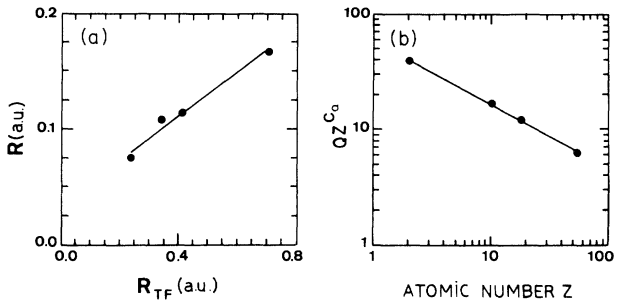

FIG. 3. (a) The parameter R of the formula of Meron and Johnson as determined from the least-squares fits of Fig. 2 vs the Thomas-Fermi radii of the noble-gas atoms. The straight line represents a least squares fit to the data points $R=0.19R_{TF}+0.03$. All quantities are expressed in atomic units. (b) The parameter QZ^{C_Q} of the formula of Meron and Johnson as determined from the least-squares fits of Fig. 2 vs atomic number Z in a double-logarithmic representation. The straight line is the result of a least-squares fit $QZ^{C_Q}=59Z^{-0.55}$.

IV) and QZ^{C_Q} were extracted from a and b by these formulas. The parameter R was plotted in Fig. 3(a) against the Thomas-Fermi radius R_{TF} of each noble gas (see Table IV for numerical values of R_{TF}). It is evident from the figure that F may be assumed to depend linearly upon R_{TF}, and a least-squares fit gave $R=0.19_{TF}+0.03$ (all quantities expressed in atomic units). In a similar way, the parameter QZ^{C_Q} was plotted in Fig. 3(b) against Z in double-logarithmic scale. Q was assumed to be independent of Z, and a power of Z was least-squares fitted to the data points in order to extract the value of the exponent C_Q. The curve shown in Fig. 3(b) is the result of this fit, which yielded $QZ^{C_Q}=59Z^{-0.55}$.

IV. CONCLUSIONS

Systematical cross-section data for the destruction of H_3^+ ions passing through noble-gas targets were obtained in the energy range from 470 to 3700 keV. The results compare well with data of other investigators, where applicable. It was observed that for a given projectile energy the destruction cross section could be scaled by a factor that depended only on the gas target. Otherwise, the destruction cross section for H_3^+ colliding with neon was compared with existing data for the H^- electron detachment cross section and for the H(1s) electron-loss cross section. The differences in absolute magnitude could be accounted for qualitatively by considering the different electron binding energies. The three processes were found to have similar velocity dependencies. This finding motivated a free-collision-model approach, originally designed for atomic projectiles, for describing the destruction of the molecular projectile H_3^+. It was subsequently demonstrated that the destruction cross sections for all noble gases studied are indeed suitably fitted by the semiempirical free-collision-model formula of Meron and Johnson using a single set of numerical values for the several parameters appearing in that formula.

ACKNOWLEDGMENTS

Three of us (W. W., L. F. S. C., and H. E. W) gratefully acknowledge the support and hospitality received from researchers and staff members of the Van de Graaf accelerator of Pontifiícia Universidade Católica at Rio de Janeiro. This work was supported in part by Financiadora de Estudos e Projetos and Conselho Nacional de Desenvolvimento Cientiífico e Tecnológico, Brazilian govermental agencies.

[1] N. V. de Castro Faria, M. J. Gaillard, J. C. Poizat, and J. Remillieux, Nucl. Instrum. Methods Phys. Res. B **43**, 1 (1989).
[2] E. E. Salpeter, Proc. Phys. Soc. (London) Ser. A **63**, 1297 (1950).
[3] K. H. Berkner, S. N. Kaplan, R. V. Pile, and J. W. Stearns, Phys. Rev. **146**, 9 (1966).
[4] M. Meron and B. M. Johnson, Phys. Rev. A **41**, 1365 (1990).
[5] M. J. Gaillard, A. G. de Pinho, J. C. Poizat, J. Remillieux, and R. Saoudi, Phys. Rev. A **28**, 1267 (1983).
[6] M. Chevallier, A. Clouvas, H. J. Frischkorn, M. J. Gaillard, J. C. Poizat, and J. Remillieux, Z. Phys. D **2**, 87 (1986).
[7] J. J. Leventhal and L. Friedmann, J. Chem. Phys. **50**, 2928 (1969).
[8] B. Peart and K. T. Dolder, J. Phys. B **7**, 1567 (1974).
[9] J. J. Soares Neto, S. Padkjaer, and J. Linderberg, Int. J. Quantum Chem.: Quantum Chem. Symp. **23**, 127 (1989).
[10] J. N. Bardsley, J. Phys. B **1**, 349 (1968).
[11] A. G. Anicich and J. H. Futrell, Int. J. Mass. Spectrom. Ion Phys. **55**, 189 (1983/1984).
[12] H. Hus, F. Youssif, A. Sen, and J. B. A. Mitchell, Phys. Rev. A **38**, 658 (1988).
[13] C. F. Fischer, *The Hartree-Fock Method for Atoms* (Wiley, New York, 1977).
[14] L. Valyi, *Atom and Ion Sources* (Wiley, London, 1977).
[15] N. Bohr and J. Lindhard, Dan. Mat. Fys. Medd. **28**, No. 7 (1954).
[16] I. S. Dmitriev and V. S. Nikolaev, Zh. Eksp. Teor. Fix. **44**, 660 (1963) [Sov. Phys.—JETP **17**, 447 (1963)].
[17] D. P. Dewangan and H. R. J. Walters, J. Phys. B **11**, 3983 (1978).
[18] D. P. Almeida, N. V. de Castro Faria, F. L. Freire, Jr., E. C. Montenegro, and A. G. de Pinho, Phys. Rev. A **36**, 16 (1987).